Negative ion chemistry in the coma of comet 1P/Halley

M. A. Cordiner & S. B. Charnley

Astrochemistry Laboratory and the Goddard Center for Astrobiology, NASA Goddard Space Flight Center, Greenbelt, MD 20770, USA

martin.cordiner@nasa.gov

Abstract

Negative ions (anions) were identified in the coma of comet 1P/Halley from in-situ measurements performed by the *Giotto* spacecraft in 1986. These anions were detected with masses in the range 7-110 amu, but with insufficient mass resolution to permit unambiguous identification. We present details of a new chemical-hydrodynamic model for the coma of comet Halley that includes – for the first time – atomic and molecular anions, in addition to a comprehensive hydrocarbon chemistry. Anion number densities are calculated as a function of radius in the coma, and compared with the *Giotto* results. Important anion production mechanisms are found to include radiative electron attachment, polar photodissociation, dissociative electron attachment, and proton transfer. The polyyne anions C_4H^- and C_6H^- are found to be likely candidates to explain the *Giotto* anion mass spectrum in the range 49-73 amu. The CN^- anion probably makes a significant contribution to the mass spectrum at 26 amu. Larger carbon-chain anions such as C_8H^- can explain the peak near 100 amu provided there is a source of large carbon-chain-bearing molecules from the cometary nucleus.

1. Introduction

Gas-phase negative ions have been detected in surprisingly large abundances during spacecraft fly-bys of Solar System bodies. During the March 1986 encounter of the *Giotto* spacecraft with the coma of comet 1P/Halley, the RPA-1 Electron Electrostatic Analyzer (EEA) detected energy spectra consistent with the presence of cold anions in the coma with masses 7-110 amu and number densities up to 1 cm^{-3} (Chaizy et al. 1991). Atomic and molecular anions O$^-$, OH$^-$, CN$^-$, C$_2$H$^-$ and larger CHON$^-$ particles were proposed by Chaizy et al. (1991) as plausible candidates to explain the observations, but due to the limited mass-resolution of the *Giotto* anion mass spectra, unambiguous identification of the detected anions was not possible. The Cassini spacecraft performed similar measurements using the CAPS Electron Spectrometer (ELS) within the atmospheres of Titan (Coates et al. 2007) and Enceladus (Coates et al. 2010), and detected negative ions with masses per unit charge ranging from ~ 10 to 10,000 amu/q.

Molecular anions were first detected in the interstellar medium using microwave spectroscopy (McCarthy et al. 2006). They have since been found to be abundant in a range of environments outside the Solar System, and are an important part of the molecular inventory of the Galaxy (Cordiner & Charnley 2012). Carbon-chain anions have been found to be abundant in quiescent molecular clouds, prestellar cores and protostars (Brünken et al. 2008, Gupta et al. 2009, Sakai et al. 2007, 2010, Cordiner et al. 2011), as well as the carbon-rich AGB star IRC+10216 (Remijan et al. 2007). Chemical models have been able to reproduce the observed anion abundances in interstellar and circumstellar environments, and have shown that molecular anions have important effects on the chemistry and ionization balance of the gas (Cordiner & Millar 2009, Walsh et al. 2009, Cordiner & Charnley 2012, McElroy et al., Forthcoming). Whereas chemical kinetic models have been successful in explaining the abundances of small molecular anions in Titan's upper atmosphere (Vuitton et al. 2009), the origin and importance of anions in the coma of comet 1P/Halley, as well as for comets in general (Wekhoff 1981),

remains to be understood.

In this article, we utilize a combined chemical/hydrodynamic model for the coma of comet Halley to explore various anion production mechanisms and compute the abundances of atomic and molecular anions as a function of radius in the coma.

2. Chemical model

Our model is based on the five-fluid coma model of Rodgers & Charnley (2002), which models the dynamics of a neutral fluid, a positively-charged fluid, an electron fluid and fluids of fast atomic and molecular hydrogen. These fluids emanate from the nucleus in a spherically-symmetric outflow (see also Rodgers et al. 2004), and the abundances of various chemical species are calculated as a function of radius. The chemical network has been fully updated in the present work and incorporates reactions between 279 chemical species (composed of H, C, N and O atoms, and electrons). The list of species consists of 154 cations, 23 anions (listed in Table 1) and 101 neutrals. Hydrocarbon chemistry is modeled for species containing up to eight C-atoms. Carbon-chain-bearing anions are included because of the importance of C_2 and C_3 in cometary comae (Weiler 2012), and because their gas-phase chemistry is better understood than other classes of anions such as PAHs. The abundances of the modeled species are linked by a total of 3823 chemical reactions, 3367 of which were taken from the latest version of the UMIST database for astrochemistry (RATE12; McElroy et al. Forthcoming), including 685 reactions involving anions.

Table 1. Anions included in the model

H^-, O^-, OH^-, O_2^-,
C^-, C_2^-, C_3^-, C_4^-, C_5^-, C_6^-, C_7^-, C_8^-,
CH^-, C_2H^-, C_3H^-, C_4H^-, C_5H^-, C_6H^-, C_7H^-, C_8H^-,
CN^-, C_3N^-, C_5N^-

Solar photo-reaction rates at 1 AU have been taken from Huebner et al (1992) and Crovisier (1994) where available. New photodissociation rates were calculated for hydrocarbons based on the cross sections of van Hemert & van Dishoeck (2008), integrated over the quiet sun solar irradiance spectrum (Woods et al. 2009). For the remaining neutral species, known photo-rates for structurally similar species were used, with product channels taken from the RATE12 database. Anion photodetachment rates were calculated using the square-root threshold law (Millar et al. 2007). We used measured cross sections above threshold for C_2H^-, C_4H^- and C_6H^- (from Best et al. 2011), and for OH^- (Trippel et al. 2006). Above-threshold photodetachment cross-sections were assumed to be 10^{-17} cm^2 for all other anions.

Mutual neutralization reactions have been included between all anions in the model and the most abundant cations, including H_2O^+, H_3O^+, NH_4^+, $C_2H_2^+$, $C_2H_4^+$, $HCNH^+$, $CH_3OH_2^+$ and $CH_3OCH_4^+$, with rate coefficients of 7.5×10^{-8} $(T_c/300)^{-0.5}$ cm^3 s^{-1}. In this formula T_c is the effective collision temperature, defined by

$$T_c = \frac{m_i T_a + m_a T_i}{m_i m_a},$$

where T_i and T_a are the respective temperatures of the (cat)ionic and anionic reactants, and m_i and m_a are their respective masses.

A further 78 reactions involving anions have been added, including proton transfer, dissociative electron attachment and polar photodissociation. A summary of the main chemical processes involving anions in the coma model is given in Table 2. The dominant anion formation processes are described in more detail in Section 3.

Table 2. Anion reaction types included in the coma model

Abbreviation	Reaction Type	Example
REA	Radiative electron attachment	$A + e^- \rightarrow A^- + h\nu$
PPD	Polar photodissociation	$AB + h\nu \rightarrow A^- + B^+$
DEA	Dissociative electron attachment	$AB + e^- \rightarrow A^- + B$
PT	Proton transfer	$AH + B^- \rightarrow A^- + BH$
MN	Mutual neutralization	$A^- + B^+ \rightarrow A + B$
AED	Associative electron detachment	$A^- + B \rightarrow AB + e^-$
AN	Anion-neutral	$A^- + B \rightarrow C^- + D$
CT	Charge transfer	$A^- + B \rightarrow A + B^-$
PD	Photodetachment	$A^- + h\nu \rightarrow A + e^-$

The contribution of anion chemistry to the energetics of the gas is negligible in the majority of models considered here due to the relatively small anion abundances. The kinetic temperature of the anions is assumed to be identical to the temperature of the neutral gas from which they are formed.

Our model for Halley assumes a spherical nucleus with radius 3.36 km, heliocentric distance 0.89 AU, temperature 192 K and H_2O production rate of $Q(H_2O) = 6.9 \times 10^{29}$ s^{-1}, appropriate to the time of the *Giotto* encounter on 13 March 1986 (Schmidt et al. 1988). Production rates of parent species are given in Table 3. These have been taken from the compilation of Haider & Bhardwaj (2005), with the addition of C_8H_2, that has been included as representative of a generic long-chain hydrocarbon molecule (see Section 5).

Table 3. Production rates for parent species relative to H_2O

| Species	Production Rate	Species	Production Rate
H_2O	1.0	C_2H_4	3.00×10^{-3}
CH_4	6.25×10^{-3}	CO	1.00×10^{-1}
NH_3	1.88×10^{-2}	C_2H_6	4.00×10^{-3}
C_2H_2	2.50×10^{-2}	CH_3OH	2.13×10^{-2}
HCN	1.25×10^{-3}	CO_2	3.75×10^{-2}
N_2	1.25×10^{-3}	C_8H_2	1.00×10^{-5}

3. Anion production processes

3.1 Radiative electron attachment

Two main processes are responsible for initiation of the anion chemistry in the inner coma (at radial distances less than ~ 1000 km from the nucleus): radiative electron attachment and polar photodissociation. As a result of their large electron affinities, combined with a high vibrational density of states, carbon-chain-bearing molecules (including polyynes, C_nH, for $n > 3$), possess the ability to attach low-energy free electrons and undergo rapid radiative relaxation to form stable anions (Herbst & Osamura 2008). As shown in Fig. 1c, the C_6H^- number density quickly reaches > 1 cm^{-3} as a result of radiative electron attachment to C_6H. The C_6H molecule is formed in the coma from electron recombination of $C_6H_4^+$ – a moderately large hydrocarbon ion that arises in the model as a product of acetylene photochemistry. The neutral-neutral reaction

$$C_2 + C_2H_2 \rightarrow C_4H + H$$
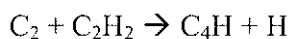
results in the formation of a large amount of C_4H (reaching a production rate of ~ $10^{-4} Q(H_2O)$). However, due to its smaller size, C_4H is theorized to possess a smaller radiative electron attachment rate than C_6H (Herbst & Osamura 2008), causing C_4H^- to be less abundant than C_6H^- in the inner coma. The larger C_8H^- anion is abundant in our model as a consequence of the inclusion of C_8H_2 as a parent. In the innermost regions of the coma (at radial distances < 10 km), where few Solar UV photons penetrate, C_8H is produced as a result of charge transfer from H^+ to C_8H_2, which forms $C_8H_2^+$ ions that undergo subsequent electron recombination to $C_8H + H$. At larger radii, photodissociation of C_8H_2 is the dominant source of C_8H.

The majority of the C_3N^- in the model comes from radiative electron attachment to C_3N, which is produced predominantly as a result of the neutral-neutral reaction

$$C_2 + HCN \rightarrow C_3N + H.$$
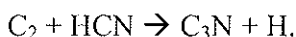
3.2 Polar photodissociation

At distances greater than ~ 10 km from the nucleus, the penetration of solar UV radiation becomes sufficiently strong that polar photodissociation (PPD) of neutral molecules becomes an important source of negative ions. Also known as threshold ion pair production, PPD is the process by which absorption of radiation by a molecule AB results in the production of a pair of oppositely-charged product species A^- and B^+ (see Table 2). Polar photodissociation of H_2O, HCN, CO and CO_2 was studied in the laboratory by Hunniford et al. (2007), Berkowitz et al. (1969), Dadouch (1991) and Mitsuke (1990), respectively. Our model incorporates rates for PPD calculated in the solar radiation field using the cross sections given by Vuitton et al. (2009), integrated over the applicable energy range for each process (taken from the original laboratory studies).
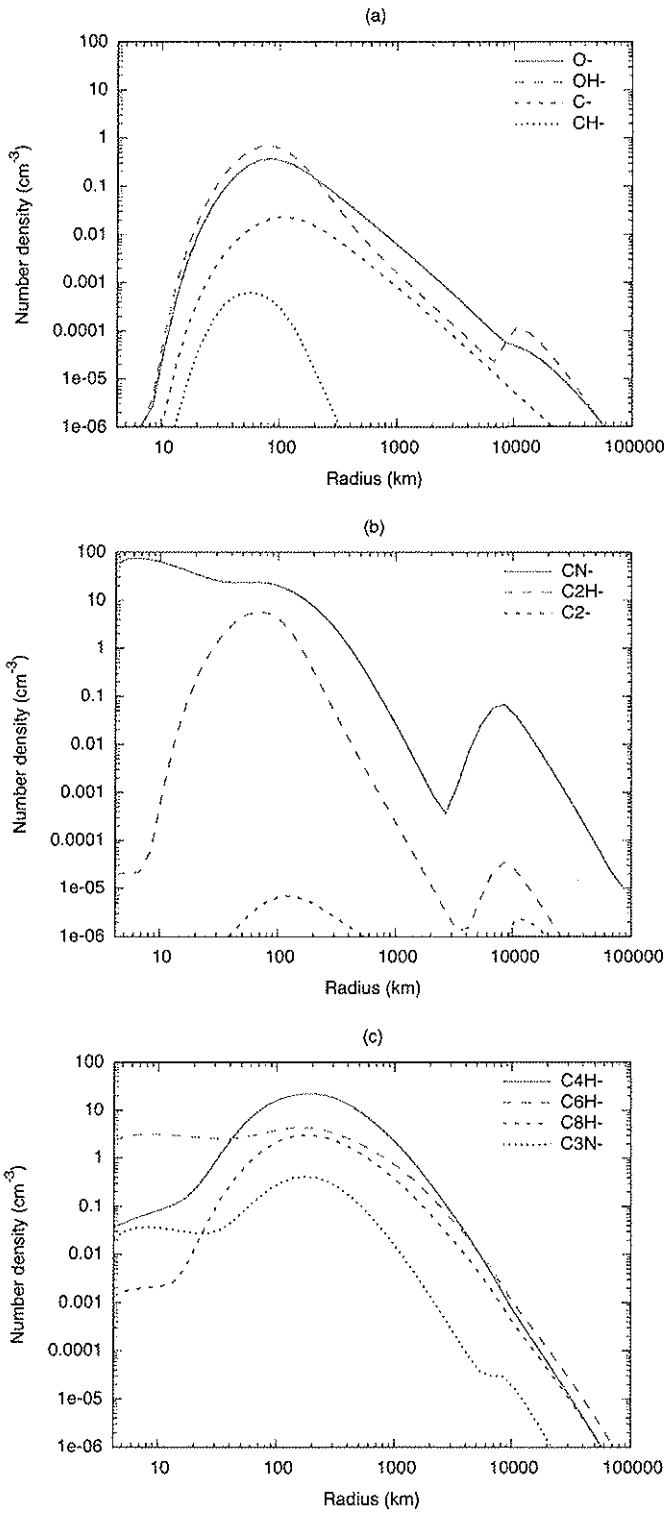
Fig. 1. Modeled negative ion (anion) number densities in the coma of comet 1P/Halley as a function of distance from the nucleus.

Polar photodissociation of H_2O by photons in the energy range 36-100 eV produces both O^- and H^- (Hunniford et al. 2007). This is the dominant production mechanism for atomic anions in our coma model. The O^- number density as a function of radius is shown in Fig. 1a, which reaches a peak value of ~ 1 cm^{-3} at a radius of ~ 80 km. Polar photodissociation of CO is the primary production mechanism for C^- throughout the coma.

3.3 Proton transfer

Polar photodissociation of HCN is an important source of CN^-, but the dominant production mechanism for this anion in our model is via loss of protons from HCN through proton-transfer reactions. The transfer of protons from neutral species to anions can be highly exoergic depending on the acidity of the neutral in question, and such reactions are almost always extremely fast in the gas phase (Vuitton et al. 2009). For the anions in our model, we have included all relevant exoergic proton transfer reactions, with rate coefficients taken from the RATE12 database and from Vuitton et al. (2009) where available. Reaction rates have been extrapolated to the additional anions in our model where necessary.

As a result of its high proton affinity, H^- quickly reacts with H_2O to produce $OH^- + H_2$. Consequently, OH^- reaches a large number density in the coma, similar to that of O^-. Abundant C_2H^- is produced by proton transfer from C_2H_2 to O^- and OH^-. Proton transfer from HCN to C_4H^- and C_6H^- is the dominant source of CN^- for radii less than $\sim 2,000$ km.

3.4 Dissociative electron attachment

For radii greater than $\sim 2,000$ km, dissociative electron attachment (DEA) to HCN is the dominant source of CN^-. The onset of this formation process manifests as the emergence of a secondary peak in the CN^- number density at around 10,000 km (see Fig. 1b), dominating over the proton transfer and polar photodissociation formation channels at these radii. Dissociative electron attachment rates have been calculated for the anions in our model by convolving the (Maxwellian) electron energy distribution with experimentally-derived cross sections for anion formation as a function of energy. References to much of the original laboratory data are summarized by Vuitton et al. (2009), who also provide the peak cross sections and energies. Additional DEA cross section data for C_2H_2, CO_2 and O_2 have been taken from May et al. (2008) and Rapp et al. (1965). Gaussian profiles have been assumed for the cross sections as a function of energy, which is a good approximation in most cases. A Gaussian FWHM of 1.0 eV has been used in the case of HC_3N (and HC_5N), for which no detailed cross section profile data have been published.

Dissociative electron attachment only becomes significant as a source of negative ions in the outer coma, where the electron energies become sufficient to overcome the energy barrier of this endothermic process. For example, DEA of HCN occurs at an electron energy of 2.5 eV, so the peak rate for CN^- formation from HCN occurs for electron temperatures $T_e = 2.9 \times 10^4$ K, but begins to become significant at $T_e > 1000$ K, when sufficient electrons possess the required 2.5 eV. Energetic electrons are produced by photo-ionization of water molecules. However, their temperatures only obtain large values in the outer coma where the lower density results in a reduction in the amount of energy lost in inelastic collisions with H_2O (Rodgers & Charnley 2002).

Secondary anion abundance peaks in the outer coma are also observed in our model for the following anions (see Fig. 1): OH^- (produced from DEA of H_2O), C_2H^-, C_2^- (from DEA of C_2H_2), and C_3N^- (from

DEA of HC_3N). Secondary DEA peaks are not seen for the larger polyyne anions (C_nH^-, for $n > 3$), because their large radiative electron attachment rates dominate the other anion formation processes.

5. Discussion

Chaizy et al. (1991) detected anions in the coma of comet Halley with masses in the range 7-110 amu, and despite the limited resolution of the mass spectra, identified three main peaks at (1) 7-19 amu, (2) 22-65 amu and (3) 85-110 amu. They referred to these as the '17 amu group', the '30 amu group' and the '100 amu group', respectively. The most likely candidate species to explain Peak 1 are shown in Fig. 1a: O^- and OH^-, C^- and CH^-. In our model, O^- is the most abundant of these anions throughout much of the coma – OH^- is slightly more abundant in the inner regions (at a radial distance $r < 200$ km from the nucleus) and outer regions ($r > 10,000$ km). Chaizy et al. (1991) derived anion number densities for Peak 1 starting at more than 1 cm^{-3} at $r = 3 \times 10^3$ km and falling to $\sim 10^{-4}$ cm^{-3} at $r \sim 3 \times 10^4$ km, (as shown in their Fig. 4). Outside of the comet's ionopause (at $r = 4,500$), our modeled Peak 1 anion abundances are about two orders of magnitude less than observed.

The mass range covered by Peak 2 contains the relatively small di/tri-atomic anions C_2^-, CN^- and C_2H^-, as well as some of the medium-sized carbon-chain-bearing anions: C_4H^- and C_3N^-. Over the range of the *Giotto* data (from $r = 3 \times 10^3$ km to 3×10^4 km), the observed Peak 2 anion densities fall from $\sim 10^{-2}$ to 10^{-5} cm^{-3}. As can be seen in Fig. 1, our modeled number densities for CN^- and C_4H^- match this trend quite well (within an order of magnitude) at all radii. Fig. 4 of Chaizy et al. (1991) shows a rise in the observed number density of these '30 amu group' anions between 1×10^4 km and 2×10^4 km, which is consistent with the location of the rise in anion abundances (including that for CN^-), which occurs as a result of DEA in the outer coma.

Peak 3 contains the larger carbon-chain-bearing anions C_6H^- and C_8H^-. Our modeled number densities for these species as a function of radius are again consistent (within an order of magnitude) with the number densities of anions in this mass range detected by *Giotto*.

The C_8H_2 molecule is included as a parent in the coma model, and is intended to be representative of the class of large carbon-chain-bearing species that could plausibly be present as a component of cometary nuclei (Mumma & Charnley 2011). Photodissociation of C_8H_2 is assumed to result in H-atom loss to produce the polyyne C_8H, although alternative product channels are possible, including loss of various numbers of carbon atoms. Long carbon chains and polyynes (including C_8H) undergo radiative electron attachment at similarly rapid rates (Herbst & Osamura 2008). Thus, C_8H^- in our model can be considered as representative of the class of anions that arise in the coma as a consequence of the release of dusty, carbon-chain-rich material from the nucleus. The appearance of a strong anion mass peak in the *Giotto* observations at ~ 100 amu is thus readily explainable. As a final point, we note that if a sufficient quantity of long carbon chains is released from the nucleus (with a production rate greater than $\sim 10^{-4} Q(H_2O)$), rapid radiative electron attachment ensues and molecular anions can be formed in such large abundances that they become the dominant carriers of negative charge in the inner coma (at distances $< 10^3$ km from the nucleus). Evidence for the presence of abundant carbon chains in Halley was provided by Geiss et al. (1999), who derived a C_4H production rate of 0.023 $Q(H_2O)$. In such a situation, the total abundance of anions is sufficiently large that their thermodynamic effects on the coma begin to become important. A proper treatment of these effects will require the inclusion of a separate anion fluid in future hydrodynamical coma models. The properties of such an anion fluid will be examined in detail by Cordiner & Charnley (Forthcoming).

The scatter on the anion number densities as a function of radius presented by Chaizy et al. (1991) is considerable, and often larger than the associated error bars. Uncertainty is inherent in their results due to the fact that the *Giotto* EESA was calibrated for use in electron spectroscopy rather than (heavy) ion spectroscopy. In fact, the efficiency of the EESA microchannel plate (MCP) detector for measuring negative ion fluxes is highly uncertain due to a lack of laboratory calibration for such purposes. Thus, the results of Chaizy et al. (1991) can only be considered approximate such that a direct quantitative comparison of our results may not be meaningful. Nevertheless, the qualitative agreement between observations and our model predictions is good, especially considering some of the uncertainties in the model. Based on laboratory measurements of polyyne anions and OH^-, the photodetachment cross sections employed for many of the other anions (including O^-, OH^-, CN^- and C_3N^-), are likely to be accurate to within a factor of a few at best. Because photodetachment is by far the dominant anion destruction mechanism, errors on these cross sections propagate in an approximately linear fashion to the modeled abundances of these species. For those species whose production is dominated by polar photodissociation, a potentially more significant source of error is the uncertainty in the PPD cross sections, which have been approximated and may only be accurate to within 1-2 orders of magnitude. Thus, we highlight a need for dedicated laboratory measurements of these values. Due to a similar lack of laboratory measurements for electron attachment to neutrals at low energies and densities, the radiative electron attachment (REA) rates for all anions in the model are based on theoretical calculations. Previous endeavors to model observed anion abundances in dark molecular clouds and circumstellar envelopes have shown that the theoretical REA rates are reasonably accurate for C_6H^- and C_8H^-, but less so for C_4H^-, the rate for which seems to have been over-estimated.

Other possible sources of uncertainty in our model include a lack of measured rate coefficients for several important proton transfer reactions, including the reactions of O^- and OH^- with C_2H_2, and the polyyne anions with HCN. In addition, our list of PPD and DEA reactions is incomplete due to a lack of laboratory studies of these processes for some abundant coma molecules such as NH_3, H_2CO and CH_3OH. Possible anionic products from PPD and DEA reactions involving these species may include NH_2^-, CH^- and CH_3O^-, respectively, which are not included in our model.

The fact that our model produces about two orders of magnitude less Peak 1 anions (O^-, OH^-) than observed may be indicative of missing formation processes for these species. For example, Chaizy et al. (1991) hypothesized that anions could be produced in high-energy collisions between neutral species in the coma. The process of anion production through collisions between neutral species at energies E up to 20 eV was reviewed by Wexler (1973). Cross sections for anion production in higher-energy impacts ($E \sim 100 - 1,000$ eV) are typically very small (McDaniel 1964), but a value of $\sim 10^{-18}$ cm^2 at $E \sim 100$-250 eV was measured by Gealy & van Zyl (1987) for anion production in collisions between H and H_2. This process could be an important source of anions in the coma given a sufficiently strong source of energetic atoms or molecules. Eviatar et al. (1989) deduced that such a flux of neutral species may be present in the coma of comet Halley in order to explain the fluxes of fast ions detected by *Giotto*. Given the dominance of water in the coma, collisional dissociation of H_2O may thus be considered a plausible source of H^-, O^- and OH^-. However, collisional dissociation of H_2O – and other abundant coma molecules – has yet to be studied in the laboratory, so the existence of these hypothetical anion production channels (not to mention their cross sections), is presently unknown.

5. Conclusion

A reasonably good agreement has been achieved between observed and modeled anion abundances in the coma of comet 1P/Halley, despite uncertainties in various cross sections and rates for anion production and destruction. The dominant anion production mechanisms are found to be polar photodissociation of water and radiative electron attachment to carbon chains in the inner coma, followed by proton transfer from C_2H_2 and HCN to produce C_2H^- and CN^-, respectively. In the outer regions of the coma where electron temperatures reach $\sim 10^3$-10^5 K, dissociative electron attachment becomes a dominant process.

We find particularly good agreement for CN^- and C_4H^- in the '30 amu group', and for C_6H^- and C_8H^- in the '100 amu group'. We thus confirm the hypothesis that CN^- is a likely carrier of the 20-30 amu anion mass peak observed by *Giotto* in the 1986 encounter with comet Halley. The polyyne anions C_4H^- and C_6H^- are likely constituents of the mass spectrum in the range 49-73 amu. Larger carbon-chain-bearing anions such as C_8^- and C_8H^- can explain the mass peak near 100 amu, provided a source of large carbon-chain-bearing molecules is present in the cometary nucleus.

If our interpretation of anion chemistry in the *Giotto* data is correct, then comets may contain significant abundances of long carbon-chain molecules. Measurements with the Ion and Electron Sensor on the Rosetta spacecraft during its scheduled 2014 encounter with comet 67P/Churyumov-Gerasimenko will provide additional insight into this issue. A more complete understanding of cometary anions will be facilitated by future laboratory measurements of absolute cross-sections for anion photodetachment and polar photodissociation of H_2O and other abundant coma molecules.

Acknowledgements

References

Berkowitz J., Chupka W. A., Walter T. A. 1969. Photoionization of HCN: The electron affinity and heat of formation of CN. Journal of Chemical Physics. 50. 4:1497

Best, T., Otto R., Trippel S., Hlavenka P., von Zastrow A., Eisenbach S., Jézouin S., Wester R., Vigren E., Hamberg M., Geppert W. D. 2011. Absolute photodetachment cross-section measurements for hydrocarbon chain anions. Astrophysical Journal. 742:63

Brünken S., Gupta H., Gottlieb C. A., McCarthy M. C., Thaddeus P. 2007. Detection of the carbon chain negative ion C_8H^- in TMC-1. Astrophysical Journal. 664:L43

Chaizy P., Reme H., Sauvaud J. A., D'Uston C., Lin R. P., Larson D. E., Mitchell D. L., Anderson K. A., Carlson C. W., Korth A., Mendis D. A. 1991. Negative ions in the coma of comet Halley. Nature. 349:393

Coates A. J., Crary F. J., Lewis G. R., Young D. T., Waite J. H. Jr, Sittler E. C. Jr. 2007. Discovery of heavy negative ions in Titan's ionosphere. Geophysical Research Letters. 34:L22103

Coates A. J., Jones G. H., Lewis G. R., Wellbrock A., Young D. T., Crary F. J., Johnson R. E., Cassidy T. A., Hill T. W. 2010. Negative ions in the Enceladus plume. Icarus. 206:618

Cordiner M. A., Millar T. J. 2009. Density-enhanced gas and dust shells in a new chemical model for IRC+10216. Astrophysical Journal. 697:68

Cordiner M. A., Charnley, S. B. 2012. Gas-grain chemical models for interstellar carbon chain anions. Astrophysical Journal. 749:120

Cordiner M. A., Charnley, S. B. Forthcoming. Astrophysical Journal

Crovisier, J. 1994. Photodestruction rates for cometary parent molecules. Journal of Geophysical Research. 99. 2:3777

Dadouch A., Dujardin G., Hellner L., Besnard-Ramage M. J. 1991. Highly excited quasistable states of neutral CO lying up to the double-ionization-energy level. Physical Review A. 43. 11:6057

Eviatar A., Goldstein R., Young D. T., Balsiger H., Rosenbauer H., Fuselier S. 1989. Energetic ion fluxes in the inner coma of comet P/Halley. Astrophysical Journal. 339:545

Gealy M. W., Van Zyl B. 1987. Cross sections for electron capture and loss. II. H impact on H and H_2. Physical Review A. 36. 7:3100

Geiss J., Altwegg K., Balsiger H., Graf S. 1999. Rare atoms, molecules and radiacals in the coma of P/Halley. Space Science Reviews. 90:253

Gupta H., Gottlieb C. A., McCarthy M. C., Thaddeus P. 2009. A survey of C_4H, C_6H and C_6H- with the Green Bank Telescope . Astrophysical Journal. 691:1494

Haider S. A., Bhardwaj A. 2005. Radial distribution of production rates, loss rates and densities corresponding to ion masses < 40 amu in the inner coma of Comet Halley: Composition and chemistry. Icarus. 177:196

Herbst E., Osamura Y. 2008. Calculations on the formation rates and mechanisms for C_nH anions in interstellar and circumstellar media. Astrophysical Journal. 679:1670

Huebner W. F., Keady J. J., Lyon, S. P. 1992. Solar Photo Rates for Planetary Atmospheres and Atmospheric Pollutants. Astrophysics and Space Science. 195:1

Hunniford C. A., Scully S. W., Dunn K. F., Latimer C. J. 2007. Fragment anion spectroscopy of water in the inner and outer valence regions. Journal of Physics B. 40:1225

May O., Fedor J., Ibanescu B. C., Allan M. 2008. Absolute cross sections for dissociative electron attachment to acetylene and diacetylene. Physical Review A. 77:040701

McCarthy M. C., Gottlieb C. A., Gupta H. C., Thaddeus P. 2006. Laboratory and astronomical identification of the negative molecular ion C_6H^-. Astrophysical Journal. 652:L141

McDaniel E. W. 1964. Collision phenomena in ionized gases. John Wiley & Sons, Inc. New York. Chap. 8.

McElroy D., Walsh C., Markwick A. J., Cordiner M. A., Millar T. J. Forthcoming. The UMIST database for astrochemistry 2012. Astrophysical Journal

Mitsuke K., Suzuki S., Imamura T., Koyano I. 1990. Negative-ion mass spectrometric study of ion-pair formation in the vacuum ultraviolet. II. Journal of Chemical Physics. 93:1710

Millar T. J., Walsh C., Cordiner M. A., Ni Chuimin R., Herbst E. 2007. Hydrocarbon anions in interstellar clouds and circumstellar envelopes. Astrophysical Journal. 662:L87

Mumma M. J., Charnley S. B. 2011. The chemical composition of comets – Emerging taxonomies and natal heritage. Annual Review of Astronomy and Astrophysics. 49:471

Rapp D., Briglia D. D. 1965. Total cross sections for ionization and attachment in gases by electron impact. II. Negative-ionformation. Journal of Chemical Physics. 43:1480

Remijan A. J., Hollis J. M., Lovas F. J. et al. 2007. Astrophysical Journal. 664:L47

Rodgers S. D., Charnley, S. B. 2002. A model of the chemistry in cometary comae: deuterated molecules. Monthly Notices of the Royal Astronomical Society. 330:660

Rodgers S. D., Charnley S. B., Huebner W. F., Boice D. C. 2004. Physical processes and chemical reactions in cometary comae. Comets II, M. C. Festou, H. U. Keller, and H. A. Weaver (eds.), University of Arizona Press, Tucson. p. 505

Sakai N., Sakai T., Osamura Y., Yamamoto S. 2007. Detection of C_6H^- toward the low-mass protostar IRAS 04368+2557 in L1527. Astrophysical Journal. 667:L65

Sakai N., Shiino T., Hirota T., Sakai T., Yamamoto S. 2010. Long carbon-chain molecules and their

anions in the starless core, Lupus-1A. Astrophysical Journal. 718:L49

Schmidt H. U., Wegman R., Huebner W. F., Boice, D. C. 1988. Cometary gas and plasma flow with detailed chemistry. Computer Physics Communications. 49:17

Trippel S., Mikosch J., Berhane R., Otto R., Weidemueller M., Wester R. 2006. Photodetachment of Cold OH- in a Multipole Ion Trap. Physical Review Letters. 97:193003

Van Hemert M. C., van Dishoeck E. F. 2008. Photodissociation of small carbonaceous molecules of astrophysical interest. Chemical Physics. 33:292

Vuitton, V., Lavvas P., Yelle R. V., Galand M., Wellbrock A., Lewis G. R., Coates A. J., Wahlund J. E. 2009. Negative ion chemistry in Titan's upper atmosphere. Planetary and Space Science. 57. 13:1558

Walsh C., Harada N., Herbst E., Millar T. J. 2009. Astrophysical Journal. 700:725

Woods T. N., Chamberlin P. C., Harder J. W., Hock R. A., Snow M., Eparvier F. G., Fontenla, J. McClintock W. E., Richard E. C. 2009. Solar Irradiance Reference Spectra (SIRS) for the 2008 Whole Heliosphere Interval (WHI). Geophysical Research Letters. 36:L01101

Weiler M. 2012. The Chemistry of C_3 and C_2 in cometary comae. Astronomy & Astrophysics. 538:A149

Wekhoff A. 1981. Negative ions in comets. The Moon and Planets. 24:157

Wexler S. 1973. Associative and non-associative ion pair formation by fast atoms. Berichte der Bunsen-Gesellschaft. 77. 8:606